Importance of Clustered 2′-*O*-(2-Aminoethyl) Residues for the Gene Targeting Activity of Triple Helix-Forming Oligonucleotides‡

Nitin Puri,§ Alokes Majumdar,§ Bernard Cuenoud,|| Paul S. Miller,⊥ and Michael M. Seidman*,§

Laboratory of Molecular Gerontology, National Institute on Aging, National Institutes of Health, Baltimore, Maryland 21224, Novartis Pharmaceuticals Ltd., 4002 Basel, Switzerland, and Department of Biochemistry and Molecular Biology, Bloomberg School of Public Health, Johns Hopkins University, Baltimore, Maryland 21205

Received October 7, 2003; Revised Manuscript Received December 2, 2003

ABSTRACT: We are developing triple helix-forming oligonucleotides (TFOs) as gene targeting reagents in living mammalian cells. We have described psoralen-linked TFOs with 2′-*O*-methyl and 2′-*O*-(2-aminoethyl) (2′-AE) substitutions that are active in a gene knockout assay in cultured cells. The assay is based on mutagenesis by psoralen, a photoactive DNA cross-linker. Previous work showed that TFOs with three or four 2′-AE residues were disproportionately more active than those with one or two substitutions. Here we demonstrate that for optimal bioactivity the 2′-AE residues must be clustered rather than dispersed. We have further characterized bioactive and inactive TFOs in an effort to identify biochemical and biophysical correlates of biological activity. While thermal stability is a standard monitor of TFO biophysical activity, we find that T_m values do not distinguish bioactive and inactive TFOs. In contrast, measurements of TFO association rates appear to correlate well with bioactivity, in that triplex formation occurs disproportionately faster with the TFOs containing three or four 2′-AE residues. We asked if extending the incubation time prior to photoactivation would enhance the bioactivity of a TFO with a slow on rate relative to the TFO with a faster association rate. However, there was no change in bioactivity differential. These results are compatible with a model in which TFO binding *in vivo* is followed by relatively rapid elution by cellular functions, similar to that described for transcription factors. Under these circumstances, TFOs with faster on rates would be favored because they would be more likely to be in triplexes at the time of photoactivation.

Reagents that could find and bind specific sequence targets in mammalian chromosomes in living cells would have enormous utility for research, commercial, and gene therapy applications. The importance of a robust gene manipulation technology is the motivation for the long-standing effort to develop triple helix-forming oligonucleotides (TFOs)[1] as gene targeting reagents (*1*−*5*). Although triplexes are the subject of an extensive biochemical and biophysical literature (*2*, *3*), it is only recently that TFOs have been shown to be capable of mediating changes in the sequence of chromosomal targets (*6*−*9*). In part, this is the result of the incorporation into TFOs of novel base or sugar analogues, such as 2′-*O*-(2-aminoethyl)ribose (2′-AE-ribose) (*7*, *8*).

Triplexes form when a third strand lies in the major groove of a polypurine·polypyrimidine duplex target, and are stabilized by two hydrogen bonds between the third-strand bases and the purines in the duplex. When the third strand consists of pyrimidines, the triplets are T·A:T and C+·G:C (*10*) (the cytosine must be protonated at N^3 to support a second Hoogsteen hydrogen bond). Triplex formation is stringent with respect to sequence, and single mismatches are destabilizing. Although the restriction to simple sequences would seem to sharply limit biological applications, such sequence elements are abundant in mammalian genomes, and many genes have appropriate sites (*11*, *12*).

There are a number of challenges to TFO bioactivity. These fall into two categories: those pertaining to the chemistry and biochemistry of the oligonucleotide and those related to the genomic target in the nuclear environment. From the perspective of TFOs in the pyrimidine motif, there are several problems, most of which have been addressed by the use of base and sugar analogues. Pyrimidine motif triplexes are unstable at physiological pH because of the requirement for cytosine protonation, which occurs at acidic pH ($pK_a = 4.5$). However, replacement of cytosine with 5-methylcytosine permits triplex formation at neutral pH (*13*). Triplex formation by deoxy TFOs imposes conformational restrictions on the third strand and requires distortion of the duplex. This has been addressed by use of third strands with 2′-*O*-methylribose sugars (*14*, *15*). Triplexes formed by 2′-OMe third strands require less distortion of the third strand and underlying duplex (*16*). These triplexes can be more stable than the underlying duplex, in contrast to those formed by deoxy third strands (*7*, *17*). The level of negative charge

‡ Dedicated to the memory of Dr. Claude Helene, the leader of our field.

* To whom correspondence should be addressed: LMG/NIA/NIH, 5600 Nathan Shock Dr., Baltimore, MD 21224. Phone: (410) 558-8565. Fax: (410) 558-8157. E-mail: seidmanm@grc.nia.nih.gov.

§ National Institutes of Health.

|| Novartis Pharmaceuticals Ltd.

⊥ Johns Hopkins University.

[1] Abbreviations: 2′-AE, 2′-*O*-(2-aminoethyl); 2′-OMe, 2′-*O*-methoxy; pso, psoralen; TFOs, triple helix-forming oligonucleotides; HPRT, hypoxanthine guanosine phosphoribosyl transferase; T_m, temperature of half-dissociation; CHO, Chinese hamster ovary.

10.1021/bi035808l CCC: $27.50
Published on Web 01/14/2004

repulsion between the phosphates of the third strand and duplex has been reduced by the use of the 2′-AE substitution, which is protonated at physiological pH (*7*, *18*, *19*). This modification, like 2′-OMe, stabilizes the C3′-endo conformation of the sugar and preorganizes the third strand into a structure similar to that found in the triplex (*16*, *18*), thus reducing some of the entropic barriers to triplex formation (*20*). Furthermore, the sugar modifications also confer some degree of nuclease resistance on the oligonucleotides.

There are other, more "biological", impediments to triplex formation and stability *in vivo*. The genomic target exists in the context of eukaryotic chromatin, which in static form blocks access to TFOs, similar to what has been described for many regulatory proteins (*21*−*23*). However, chromatin structure is dynamic as a function of the cell cycle, transcription, replication, and DNA repair (*24*−*26*). This allows target recognition by sequence specific binding proteins and, presumably, TFOs. Thus, at the time of TFO introduction, the accessibility of the target sequence will reflect the biology of the cell and the metabolism of the gene in which the target resides. For example, we have found much greater target access in S phase cells than in quiescent cells (*8*). Transcription can also open access to targets (*27*). Another concern is the residence time of the TFO after binding *in vivo*. To a certain extent, this will simply reflect the intrinsic off rate of the TFO as measured in conventional biochemical assays. However, we have shown that preformed triplexes are much less stable following introduction into cells than would be predicted by *in vitro* analyses (*28*, *29*). Triplexes can be unwound by helicases (*30*, *31*) and by translocases found in chromatin remodeling complexes (*32*), and these may destabilize triplexes in the cell.

The biological activity of a TFO against a specific target *in vivo* is, then, a complex function of multiple parameters. Development of reliable gene targeting protocols will require effective TFO chemistry, as well as an understanding and manipulation of the target biology. In previous work, we identified TFOs containing a patch of 2′-AE residues that were active in the *hprt* knockout assay (*7*). In this report, we have articulated further the contribution of 2′-AE residues to TFO bioactivity. In addition, by analysis of two closely related TFOs, which form triplexes of similar thermal stability, but show quite different efficacy in biological assays, we have attempted to improve our understanding of the biophysical parameters that underlie TFO bioactivity.

MATERIALS AND METHODS

Synthesis and Purification of TFOs. 5′-*O*-(4,4′-Dimethoxytrityl)-5-methyluridine-2′-*O*-methyl-3′-*O*-(β-cyanoethyl-*N*,*N*-diisopropyl)phosphoramidite, N^4-formamidine-5′-*O*-(4,4′-dimethoxytrityl)-5-methylcytidine-2′-*O*-methyl-3′-*O*-(β-cyanoethyl-*N*,*N*-diisopropyl)phosphoramidite, the 5′-*O*-(4,4′-dimethoxytrityl)-5-methyluridine-2′-*O*-methyl-3′-*O*-succinamido-N^6-hexanamido-N^3-propyl-controlled pore glass (CPG) support, and 6-[4′-(hydroxymethyl)-4,5′,8-trimethylpsoralen]hexyl-1-*O*-(β-cyanoethyl-*N*,*N*-diisopropyl)phosphoramidite were purchased from Chemgenes (Ashland, MA). For the synthesis of 5′-*O*-(4,4′-dimethoxytrityl)-5-methyluridine-2′-*O*-(2-aminoethyl)-3′-*O*-(β-cyanoethyl-*N*,*N*-diisopropyl)phosphoramidite and N^4-(*N*-methylpyrrolidineamidine)-5′-*O*-(4,4′-dimethoxytrityl)-5-methylcytidine-2′-*O*-(2-aminoethyl)-3′-*O*-(β-cyanoethyl-*N*,*N*-diisopropyl)phosphoramidite, procedures reported previously were followed (*18*, *19*, *33*). The oligonucleotides were synthesized on CPG supports (500 Å) using an Expedite 8909 synthesizer as previously described (*29*).

Deprotection and Purification of TFOs. For the gas phase deprotection, the controlled pore glass support with pso-TFO was taken in a vial closed with a porous filter cap. The vial was placed in an enclosed steel pressure chamber with a valve and evacuated with a house vacuum. The valve was then connected to the gas cylinder, keeping the steel chamber under reduced pressure. The chamber was incubated with anhydrous methylamine gas (Aldrich) at room temperature for 30 min. This was followed by the release of the methylamine gas. The TFO was then taken up in distilled water. Analytical and semipreparative anion exchange (IE)-HPLC were carried out using a Dionex DNAPac PA-100 column (4.0 mm × 250 mm and 9.0 mm × 250 mm, respectively) on a Shimadzu HPLC system (LC-10ADvp) with a dual-wavelength detector (SPD-10AVvp) and an autoinjector (SIL-10ADvp). The column was eluted using linear gradients of sodium chloride (from 0 to 1.0 M) in 0.1 M Tris buffer (pH 7.0) at a flow rate of 1.0 mL/min and monitored at wavelengths of 254 and 315 nm (λ_{max} for psoralen). The purified oligos were characterized by capillary zone electrophoresis and matrix-assisted laser desorption time of flight mass spectroscopy.

Thermal Denaturation Experiments. The TFO and the constituent strands of the target duplexes (5′ TCAGAAGAAAAAAGAGAAA and 5′ TTTCTCTTTTTTCTTCTGA) were dissolved in buffers containing 50 mM Tris, 100 mM sodium chloride, and 2 mM magnesium chloride (pH 6.0, 6.5, 7.0, and 7.5). The solution was heated at 80 °C for 3 min and allowed to come to room temperature over the course of 30 min. The TFO/duplex target solution was incubated at 4 °C overnight. In control experiments, we found that denaturation profiles of triplexes prepared by adding the third strand to a previously prepared duplex were indistinguishable from those prepared by mixing all three strands followed by cooling. The thermal denaturation experiments were carried out using a Cary 3E UV−vis spectrophotometer fitted with a thermostated sample holder and temperature controller. Triplexes were heated from 10 to 85 °C at a rate of 0.4 °C/min, and the absorbance at 260 nm was recorded as a function of the temperature. All analyses were performed at least two times with an error of no more than 0.5 °C.

TFO Association Analysis by Absorbance Decay. The TFO + duplex → triplex transition is accompanied by decrease in UV absorbance. This decay curve has been exploited for estimating TFO association rates with the target duplex (*34*, *35*). For our experiments, the duplex strand was formed in kinetics buffer I [1 mM $MgCl_2$, 10 mM sodium cacodylate (pH 7.2), and 150 mM KCl] to give a final concentration of 1 or 2 μM (see Figure 5). One milliliter of the duplex stock solution was monitored by UV in a cuvette at 25 °C and gave a horizontal line as a function of time. The analyses were carried out at 25 °C (using a Peltier temperature controller). An aliquot of the TFO stock solution in kinetics buffer I was added with vigorous mixing to 1 mL of the duplex stock solution. The mixing process took less than 10 s. The experiments were carried out on a Cary dual-beam spectrophotometer. The decay curves were fit using second-order kinetics with the software supplied with the instrument.

Rate constants were reported as an average of three or more experiments. For comparison, the decay curves were normalized.

Cells and Synchronization Protocol. Chinese hamster ovary (CHO) AA8 cells (ATCC) were grown in Dulbecco's modified Eagle's medium (Life Technologies), supplemented with 10% fetal calf serum (FBS), penicillin, and streptomycin. Prior to an experiment, the cells were grown in HAT medium (10^{-4} M hypoxanthine, 5×10^{-5} M aminopterin, and 10^{-5} M thymidine) for 1 week to eliminate *hprt*$^-$ cells. The cells were synchronized in the G_0/G_1 phase by a variation of the method described by Sawai et al. (*36*). Briefly, cells were plated at subconfluent levels, and the next day the medium was changed to DMEM with 2% FBS and 2% DMSO. After 48 h, the cells were washed and incubated with complete medium containing 100 μM mimosine for 16 h to block them in the early S phase (~90% early S cells) (*37*). After 16 h, the cells were released from the mimosine block by feeding with DMEM and 10% FBS and further incubated for 4 h. In previous work, we have shown that the *hprt* target is most accessible in cells in the mid-S phase (*8*). Consequently, all bioactivity assays were carried out with mid-S phase cells.

TFO Electroporation, Psoralen Treatment, and hprt Mutation Assay. Mid-S phase cells were suspended at a density of 10^7 cells/mL and mixed with TFO at 5 μM. The cells were electroporated (Amaxa), followed by incubation at room temperature for 3 h, and a 3 min exposure in a Rayonet chamber to UVA light at 1.8 J/cm^2. The electroporation conditions were chosen to minimize cell toxicity (trypan blue staining showed ~95% viable cells after UVA treatment). Cells treated with free psoralen were incubated with 5 μM psoralen for 30 min, followed by UVA treatment. The cells were cultured for 8 days and then exposed to thioguanine (TG) selection (*29*).

Restriction Resistance Analysis of Nonselected Clones. Following TFO electroporation, UVA treatment, and culture for 3−5 days to permit mutagenesis, 100 cells were plated in 60 mm dishes in standard growth medium. Individual colonies were expanded, and the DNA was extracted. The I4E5 target region was amplified followed by digestion of the PCR products with *Xba*I. Digestion resistant PCR fragments were reamplified, and sequence analysis was performed.

RESULTS

The sequence and modification patterns of the TFOs are depicted in Figure 1. They were linked to psoralen and designed to target a site adjacent to exon 5 in the Chinese hamster *hprt* gene. The site terminates in 5′ TA, which is a preferred site for psoralen cross-linking. The cross-link site is also included in the recognition sequence for the *Xba*I restriction enzyme. Some of the TFOs are new to this report (AE-09, -10, and -11), while others have been described previously (AE-04, -05, -06, and -07 and PS-01) (*7*). In our earlier study, we found that TFOs with one or two 2′-AE substitutions were only marginally more active than the TFO without 2′-AE residues in the *hprt* knockout assay. However, the TFOs with three and four 2′-AE substitutions (AE-06 and AE-07, respectively) exhibited 10−15-fold greater activity, indicating that a threshold had been crossed. AE-06 and AE-07 contained contiguous 2′-AE residues at the 3′ end of the oligonucleotide. In the initial experiments in this study, we wanted to determine the influence on bioactivity of the placement of 2′-AE residues in patches at the 5′ end of the TFO (AE-09), in the middle (AE-10), or dispersed throughout the oligonucleotide (AE-11).

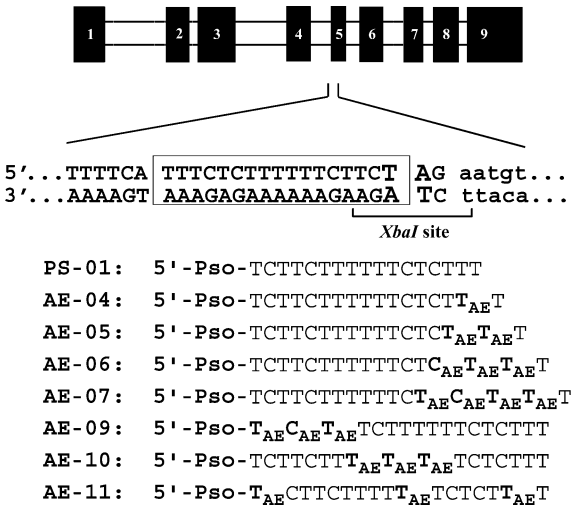

FIGURE 1: Triplex target sequence in the hamster *hprt* gene. The target lies adjacent to exon 5 (lowercase letters). The psoralen cross-link site 5′ TA lies in the recognition sequence for the *Xba*I restriction enzyme. The organization of the TFOs is shown; all sugars were 2′-OMe unless indicated as 2′-AE. All oligonucleotides were linked to psoralen.

Thermal Stability Analyses of TFOs. The triplexes formed by the TFOs were characterized by thermal stability analysis at different pH values. There was relatively little difference in the stability of the triplexes formed by the different TFOs (Supporting Information). Although there was a decline in T_m as the pH increased, in all cases the triplexes melted with a single transition (71−73 °C, pH 7.0) well above the T_m of the underlying duplex (55 °C) (*7*). Thus, the location of a patch of 2′-AE residues did not influence the thermal stability. Furthermore, the dispersal of the 2′-AE substitutions also did not have a very pronounced effect, as this triplex was only slightly less stable than the others. The T_m values, at pH 7.0, are presented in Figure 2a. For comparison, the values for the TFOs containing different numbers of 2′-AE residues are shown, presented as a function of 2′-AE content (Figure 2b). The complete set of T_m values versus pH is given in the Supporting Information.

Biological Activity of TFOs. The bioactivity of the TFOs was measured in the *hprt* knockout assay described in our previous publications (*7*). The number of colonies resistant to the thioguanine selection agent is a measure of the number of inactivating mutations in the *hprt* gene. In turn, this reflects the activity of the TFO in delivering psoralen to the target site. The TFOs with the patch of 2′-AE residues at the 3′ or 5′ end had similar activity, while placement in the middle was not quite as effective (Figure 3). The TFO with the dispersed substitutions (AE-11) was markedly less active than the others. Thus, clustering of the 2′-AE residues was important for activity.

The results presented here, and previously (*7*), describe the number and distribution of 2′-AE residues that are required for TFO bioactivity. Although our conclusions have been derived empirically, they are consistent with suggestions

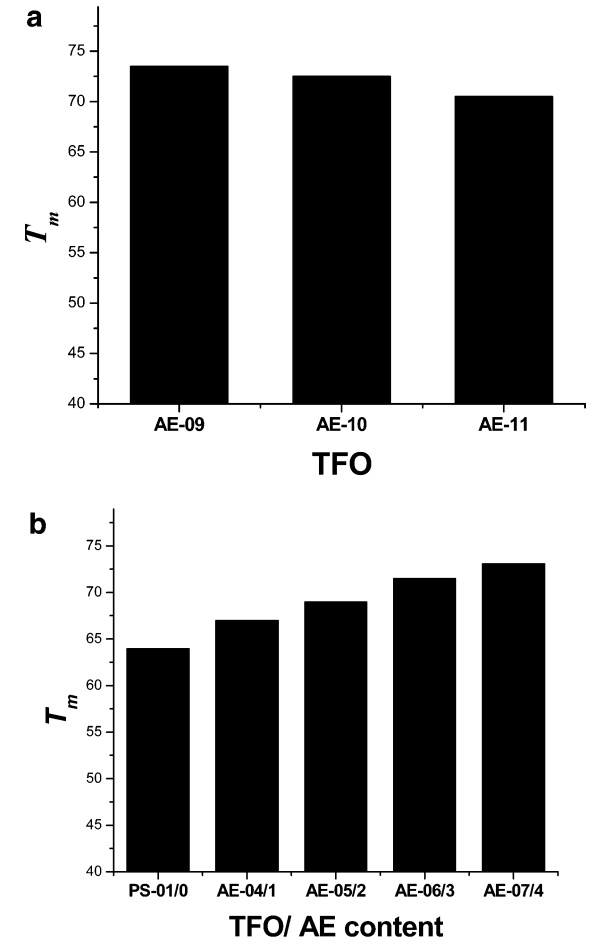

FIGURE 2: (a) Thermal stability analysis of triplexes formed by 2′-AE TFOs. The T_m (degrees Celsius) is shown for TFOs with three adjacent or dispersed 2′-AE residues. (b) Thermal stability analyses of triplexes formed by TFOs containing clustered 2′-AE substitutions at the 3′ end.

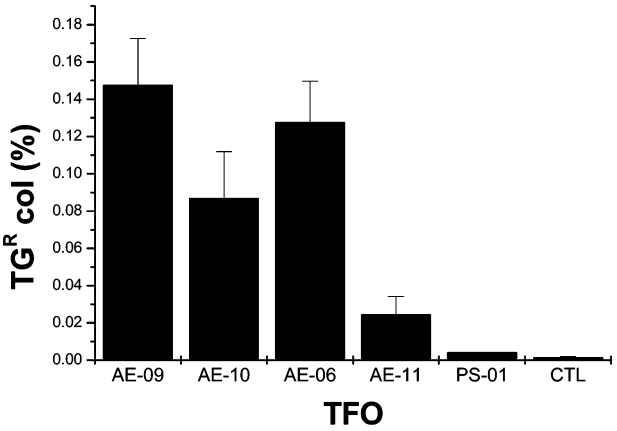

FIGURE 3: Bioactivity of AE TFOs measured in the *hprt* mutation assay. The TFOs were introduced by electroporation into hamster cells; the psoralen was photoactivated, and the frequency of cells with mutations in the *hprt* gene was determined by selection in 6-thioguanine.

in the extensive biochemical and biophysical literature about the properties of pyrimidine motif TFOs that would be necessary for bioactivity (able to form triplexes at a physiological pH and Mg^{2+} concentration, etc.). However, our T_m analysis did not predict the discontinuity in bioactivity that distinguished TFOs with three or four clustered 2′-AE residues from those with two residues or the dispersed substitution pattern (*7*). It seems likely that a TFO faces challenges *in vivo* that are not completely described by thermal stability measurements. In the following experiments, we have tried to gain some insight into the features that distinguish two TFOs containing clustered 2′-AE substitutions: the bioactive AE-07 (four 2′-AE residues) and the low-activity AE-05 (two 2′-AE residues). We chose to study these because AE-07 exhibited activity similar to that of AE-09, but was easier to synthesize with active psoralen (the proximity of the AE residues and the psoralen in AE-09 presented some problems during deprotection, the time at which psoralen is most likely to be inactivated). Furthermore, the AE patch is at the 3′ end of the TFO in both AE-05 and AE-07.

Mutagenic Activity of AE-05 and AE-07. Our conclusions about TFO bioactivity rest on a key assumption about the results of the mutagenesis assay. Psoralen-linked TFOs AE-05 and AE-07 could display quite different activities as mutagens because of an intrinsic difference in their ability to find and bind target sequences *in vivo*. Alternatively, they might differ in mutagenic potency following triplex and cross-link formation. Since we have assumed the former explanation in our assessment of TFO activity, we felt it important to examine the merits of the latter possibility. Triplexes were prepared with the two TFOs and a replication competent shuttle vector plasmid, psupF12, which contains the hamster *hprt* triplex target sequence, including the psoralen cross-link site, embedded in a variant *supF* mutation reporter gene (*29*). The triplexes were formed by overnight incubation of the plasmid with saturating amounts of TFO. UVA treatment resulted in cross-linking of >95% of the plasmids, which were then introduced into cells. After 48 h to allow for repair, mutagenesis, and replication, the progeny plasmids were harvested. The frequency of plasmids with mutations in the *supF* gene was determined in a microbiological screen (*38*). We found that the mutation frequency in the two plasmid preparations was similar: 13% for AE-05 and 14.4% for AE-07. This suggested that the TFO−psoralen cross-links formed by the two oligonucleotides were equally mutagenic, at least as assayed with the shuttle vector.

We then asked if our measurement of the mutation frequency disparity in the *hprt* assay, monitored by the thioguanine selection assay, accurately reflected the generation of all chromosomal mutations by both TFOs. The conclusion that TFOs with a patch of three or four 2′-AE residues were disproportionately more bioactive than the TFO with one or two residues was based on results of the classical thioguanine selection for cells with mutations that inactivate the *hprt* gene. Typically, these mutations are deletions that remove a portion of the triplex target and extend into exon 5, located immediately adjacent to the cross-link site (*6*, *29*). However, we have recently found that the pso-TFOs also induced base substitution mutations at the cross-link site. These do not inactivate the gene, and are not detected by thioguanine selection (*8*). They can be identified and quantitated by challenge of PCR fragments of the target region with *Xba*I, whose recognition sequence includes the cross-link site (see Figure 1). Thus, we were concerned that the low activity of the TFO with only two 2′-AE residues may have been illusory, due to the incomplete reporting of the thioguanine assay. To test this possibility, we chose colonies at random, without selection, following treatment

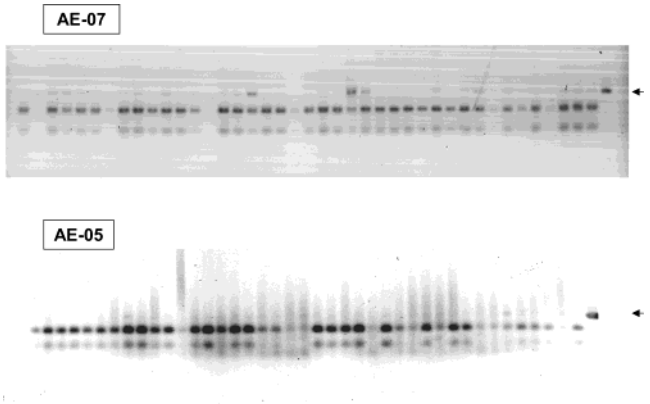

FIGURE 4: Analysis of base substitution frequency in PCR fragments of the TFO target region from nonselected, TFO-treated, cells. PCR products were analyzed by two rounds of digestion with *Xba*I and the resistant fragments further characterized by sequence analysis. The arrow marks the position of the digestion resistant fragment with the mobility of the marker in the right-most lane.

of cells with either AE-05 or AE-07. We amplified the target region and digested the fragments with *Xba*I. Resistant fragments were reamplified and redigested to eliminate false positives. Four resistant fragments were recovered from the PCR products from 92 colonies from the AE-07 treatment, while none were found in PCR products from 182 colonies treated with AE-05 (see Figure 4 for the results of the first screen). Sequence analysis showed that the *Xba*I resistant fragments had T → C changes at the 5′ T of the cross-link site. Although this was not an exhaustive study, these results supported the earlier conclusion that AE-05 was much less active than AE-07, as a gene targeting reagent.

Association Kinetics of Triplex Formation by 2′-AE TFOs. The T_m data in Figure 2b demonstrate that this classical measure of triplex stability exhibited only incremental differences between bioactive TFOs (AE-06 and -07) and those with greatly reduced activity (AE-05 and PS-01). We were interested in finding a biophysical measure of TFO activity that would give a better correlation with the bioactivity data. We decided to ask if the association rates for triplex formation, as a function of 2′-AE content, would provide that correlation. We monitored the decay over time of the ultraviolet absorbance following the addition of a third strand to a solution containing the duplex target (*34*, *35*, *39*). A representative profile in Figure 5a shows the difference between TFOs with a patch of two and four 2′-AE substitutions. The comparison of k_{on} versus 2′-AE content for all the TFOs is shown (Figure 5b). These measurements were taken with the concentration of both duplex and TFO set at 2 μM. The results of these experiments indicated that there was a continuum in the increase in association rates as the 2′-AE content increased from zero to two, and then to the dispersed three. However, there was a discontinuity going from two to three or four 2′-AE residues. This discontinuity in a biochemical parameter was concordant with the discontinuity in the measurement of bioactivity of AE-05 and AE-07.

Under the conditions of this experiment, there was an ~4-fold difference in the k_{on} values of AE-05 and AE-07. However, as reported by us previously (*7*), and confirmed in many experiments since then, the bioactivity differential between the two TFOs is on the order of 10-fold (see below).

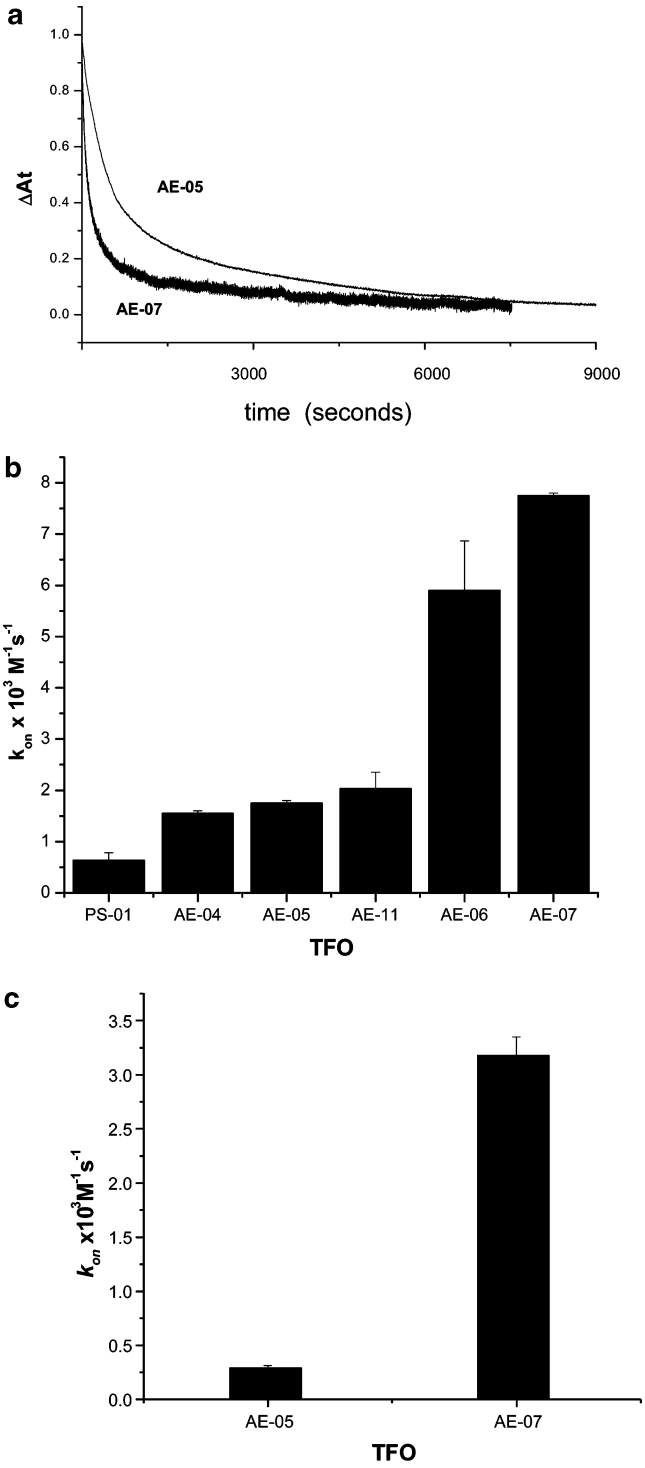

FIGURE 5: (a) Absorbance decay curves for triplex formation by AE-05 and AE-07. Duplex and TFO were mixed (2 μM each) at 25 °C in kinetics buffer I [1 mM $MgCl_2$, 10 mM sodium cacodylate (pH 7.2), and 150 mM KCl]. (b) Relative association rates vs 2′-AE content. D-3 refers to AE-11 with three dispersed AE residues. (c) Relative association rates of AE-05 and AE-07 with 1 μM TFO and duplex.

One of the goals of our research is to identify biochemical or biophysical measures of TFO activity that correlate with the bioactivity measurements. Such analyses might have predictive value for identifying bioactive TFOs. The association rate assay is sensitive to parameters such as temperature and the concentrations of the duplex and TFO. Since the results shown in this experiment demonstrated a clear

distinction between AE-05 and AE-07, it seemed possible that adjustment of the conditions of the assay might result in values of k_{on} for the two oligonucleotides that reflected the 10-fold difference seen in the bioassay. After some experimentation, we found that reducing the concentration of both the duplex and TFO to 1 μM resulted in association rates that quantitatively distinguished the two oligonucleotides in a manner similar to the biological assay (Figure 5c). The choice of these conditions was entirely arbitrary, and they bear no necessary relationship to those encountered in the nucleus by the TFOs. However, the good correlation between the results of the two quite different assays raised the possibility that the association rate of a TFO could be an important determinant of activity in chromosomal targeting *in vivo*.

Time Course of Mutagenesis. The bioassay measures the extent of *hprt* mutagenesis provoked by psoralen cross-links following triplex formation *in vivo*. After electroporation of the TFO, the cells are incubated before photoactivation of the psoralen. Only those targets with an assembled triplex at the time of photoactivation will be cross-linked and thus candidates for mutagenesis. Triplexes that form after the exposure to UVA do not contribute to the mutation frequency. In light of the results in Figure 5, we were interested in asking if our experimental protocol could be manipulated to enhance the bioactivity of a slower TFO, such as AE-05. Given the similar thermal stability of triplexes formed by AE-05 and AE-07, one possible strategy for compensating for the slower association rate of AE-05 would be to allow this TFO more time *in vivo* before its UVA treatment. Accordingly, we performed a time course experiment in which AE-05 and AE-07 were introduced into the cells followed by photoactivation at 30, 60, 180, and 360 min. The results of this experiment showed that extending the time prior to photoactivation did not increase the mutation frequency in the cultures treated with AE-05 to the levels seen with AE-07 (Figure 6a,b). Instead, the 3 h incubation was optimal for both oligonucleotides, with little difference after 6 h. The maintenance of the mutation signal after 6 h for both TFOs argued against extensive degradation of the TFOs during the incubation, and suggested that triplex formation was at steady state during the 3−6 h period.

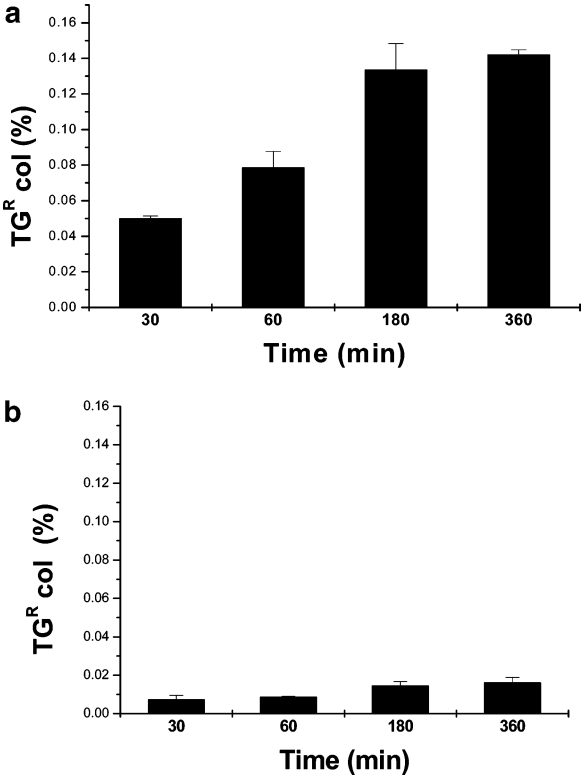

FIGURE 6: *hprt* mutation frequency of cells photoactivated at different times following introduction of AE-07 (a) or AE-05 (b).

DISCUSSION

The goal of our studies reported here and in previous publications is the development of TFOs with practical biological activity. The AE-06 and AE-07 TFOs appear to be effective reagents as determined in the *hprt* mutation assay. As we have shown with AE-07 in S phase cells, targeted mutagenesis occurs in ~5% of the cells (Figure 4), while targeted cross-link formation occurs in 20−30% of the cells (*8*). This is a level of activity sufficient for a variety of applications, such as targeted mutagenesis and studying repair of targeted adducts. Understanding the parameters that distinguish an active TFO from an inactive TFO is important for developing improved oligonucleotides, and may be informative with regard to the obstacles to TFO targeting activity at chromosomal loci in living cells.

The 2′-AE modification was first described by Cuenoud and co-workers (*18*), who showed that it conferred enhanced rates of association and increased triplex stability. At physiological pH, it introduces a local positive charge to the oligonucleotide, which partially ameliorates the charge repulsion between the third strand and the duplex. The significance of the charge repulsion problem has been appreciated for many years, and is addressed *in vitro* by including relatively high levels of divalent cations such as Mg^{2+} (*40*). Although the high levels of Mg^{2+} are very useful *in vitro*, intracellular levels of free Mg^{2+} are thought to be much lower than those commonly employed in biochemical experiments (*41*). Furthermore, molecular modeling and NMR analyses showed a specific interaction between an aminoethoxy proton and the $i - 1$ phosphate in the purine strand of the duplex, which further enhanced the stability of these triplexes (*42*). TFOs with extensive 2′-AE substitutions had very fast association rates (*18*), and it might have been expected that fully substituted TFOs would have the greatest bioactivity. However, in our initial study of TFOs with different levels of this modification, we found that extensive substitution was counterproductive insofar as biological activity was concerned (*29*). We believe that the resultant molecules may have been too "sticky" to be effective *in vivo*. Instead, as shown here and previously (*7*), a cluster of three or four 2′-AE residues is necessary and sufficient for bioactivity.

Triplex formation occurs as a result of a nucleation−elongation process similar to that described for duplex formation (*20*, *43*, *44*). The nucleus is thought to consist of three to five triplets (*34*, *43*). Nucleation is followed by either dissociation or completion by a zipper mechanism. Our association rate data indicate that the TFOs with three or four 2′-AE residues have a disproportionately faster rate of triplex formation than the TFOs with fewer substitutions or three dispersed residues. We suggest that the similarity in the number of nucleotides involved in nucleation and the

size of the 2′-AE patch in the successful TFOs is not coincidental. Instead, it seems likely that the clustering stimulates the rate of triplex formation at the nucleation step. Presumably, this results from a reduction in the level of local charge repulsion between the nucleating patch and the duplex target, and the stabilization of nucleation by the interaction of the amine and the phosphate of the purine strand of the duplex. The relationship between (clustered) 2′-AE content and association rate appears to be similar to that between 2′-AE content and bioactivity, in that both exhibit a discontinuity between two and three or four substitutions. Under appropriate conditions, the rate determination correlates very well with the differences in biological activity between AE-05 and AE-07. Since our T_m data show only incremental differences between the TFOs, it would seem that the relative association rate is a better correlate of TFO bioactivity. In our earlier study, we measured dissociation constants for these TFOs. We found a simple decrease (higher affinity) in K_D as a function of AE content when the assays were performed in 10 mM $MgCl_2$ (*7*). However, when the $MgCl_2$ concentration was lowered to 1 mM, there was a discontinuity between AE-05 and AE-06, although not as pronounced as in the on rate determinations presented here.

The mutation bioassay reflects the number of TFO−psoralen cross-links introduced at the target site. This in turn is a measure of the number of those triplexes formed by the pso-TFOs at the time of photoactivation. Triplexes assembled after the photoactivation would not produce cross-links. There are several different factors that could influence the frequency of triplex formation. The TFO must enter the cell, and nucleus, and be sufficiently stable to maintain an effective concentration during the pre-photoactivation period. The target sequence must be accessible, an important consideration given the well-established inhibition of triplex formation on nucleosomal targets (*22*). In a previous study, we argued that target accessibility could be influenced by the biological status of the cell, and we conducted the biological experiments presented here under conditions of optimal target access (*8*). Given an accessible target, why would the association rate be important for bioactivity? Posing the question assumes that this measurement, taken under arbitrary experimental conditions, is relevant to the situation *in vivo*. Given that caveat, we can consider some scenarios. One view of the extent of target occupancy by the TFO at the time of photoactivation is that it is a simple function of the biophysical properties of the oligonucleotide. Thus, given the similar stability of triplexes formed by the two TFOs, with sufficient time one would expect that the extent of triplex formation by AE-05 and AE-07 would also be similar. However, extending the time of incubation before UVA treatment did not change the bioactivity differential between the two TFOs. Consequently, it seems likely that this view is incorrect.

The preceding argument is based on the assumption that triplex stability *in vivo* reflects the *in vitro* measurement. However, if this assumption is wrong, then chromosomal triplexes might be much less stable *in vivo* than predicted by *in vitro* analyses. For example, in an earlier study with a shuttle vector model, we found that triplexes formed *in vitro* had *in vivo* residence times much shorter than expected from our biochemical analyses (*25*). We concluded that there was likely to be an active, cellular, process that destabilized triplexes following formation. Under such circumstances, the bioassay would favor the TFO with the greatest probability of rebinding, i.e., the TFO with the fastest k_{on}.

Recent studies with fluorescently tagged transcriptional regulatory proteins show that the off rates for binding of these proteins are much faster than predicted by *in vitro* measurements (*45*−*47*). It has been suggested that chromatin remodeling complexes remove sequence specific proteins (many of them binding in the major groove) from their chromosomal binding sites (*48*). Chromatin remodeling complexes can act as DNA translocases that can displace bound proteins as well as a third strand from a DNA triplex (*32*, *49*). Thus, binding of many regulatory proteins to target sites is followed by elution of the bound molecule by an active, energy-dependent process. The current view is of a dynamic system in which some proteins may spend only seconds or minutes in residence before displacement (*50*). It seems reasonable to consider binding of the third strand at chromosomal targets as an equally dynamic process, in which TFO residence time is modulated largely by cellular activities, rather than by oligonucleotide chemistry.

Some testable predictions emerge from these considerations. One is that there might be treatments of the cells that enhance triplex stability by reducing the activity of energy-dependent destabilizing factors (*51*). If this were possible, then TFOs with slower association rates might exhibit greater activity with longer incubations before photoactivation. The second is that modifications that permit TFOs to form triplexes more stable than AE-06 and AE-07 will not make an effective contribution to bioactivity unless they also improve association rates. Of course it will be of interest to ask if association rate measurements for new TFOs, under the conditions described in the legend of Figure 5c, continue to correlate with bioactivity. Finally, it may be possible to develop TFOs with faster association kinetics that would be more bioactive than those described here. Since localized positive charge appears to be important, other positively charged base, sugar, or backbone modifications might be efficacious (*9*, *52*−*54*). Similarly, compounds that enhance the kinetics of triplex formation might also be effective in cotreatment protocols (*35*). These considerations may also be important for the development of base analogues for expanding triplex target options (*55*). Eventually, of course, other factors, such as target accessibility, would limit TFO activity. However, it is likely that there is still opportunity for improvement based on chemical modifications.

ACKNOWLEDGMENT

We thank Dr. Donald Rau for helpful discussion and JiLan Liu for technical assistance.

SUPPORTING INFORMATION AVAILABLE

T_m values for triplexes formed by 2′-AE TFOs as a function of pH. This material is available free of charge via the Internet at http://pubs.acs.org.

REFERENCES

1. Felsenfeld, G., Davies, D. R., and Rich, A. (1957) Formation of a three stranded polynucleotide molecule, *J. Am. Chem. Soc. 79*, 2023−2024.

2. Thuong, N. T., and Helene, C. (1993) Sequence specific recognition and modification of double helical DNA by oligonucleotides, *Angew. Chem., Int. Ed. 32*, 666−690.
3. Radhakrishnan, I., and Patel, D. J. (1994) DNA triplexes: solution structures, hydration sites, energetics, interactions, and function, *Biochemistry 33*, 11405−11416.
4. Vasquez, K. M., and Wilson, J. H. (2000) Triplex-directed site-specific genome modification, *Methods Mol. Biol. 133*, 183−200.
5. Moser, H. E., and Dervan, P. B. (1987) Sequence-specific cleavage of double helical DNA by triple helix formation, *Science 238*, 645−650.
6. Majumdar, A., Khorlin, A., Dyatkina, N., Lin, F. L., Powell, J., Liu, J., Fei, Z., Khripine, Y., Watanabe, K. A., George, J., Glazer, P. M., and Seidman, M. M. (1998) Targeted gene knockout mediated by triple helix forming oligonucleotides, *Nat. Genet. 20*, 212−214.
7. Puri, N., Majumdar, A., Cuenoud, B., Natt, F., Martin, P., Boyd, A., Miller, P. S., and Seidman, M. M. (2002) Minimum Number of 2′-O-(2-Aminoethyl) Residues Required for Gene Knockout Activity by Triple Helix Forming Oligonucleotides, *Biochemistry 41*, 7716−7724.
8. Majumdar, A., Puri, N., Cuenoud, B., Natt, F., Martin, P., Khorlin, A., Dyatkina, N., George, A. J., Miller, P. S., and Seidman, M. M. (2003) Cell Cycle Modulation of Gene Targeting by a Triple Helix-forming Oligonucleotide, *J. Biol. Chem. 278*, 11072−11077.
9. Vasquez, K. M., Dagle, J. M., Weeks, D. L., and Glazer, P. M. (2001) Chromosome targeting at short polypurine sites by cationic triplex-forming oligonucleotides, *J. Biol. Chem. 276*, 38536−38541.
10. Letai, A. G., Palladino, M. A., Fromm, E., Rizzo, V., and Fresco, J. R. (1988) Specificity in formation of triple-stranded nucleic acid helical complexes: studies with agarose-linked polyribonucleotide affinity columns, *Biochemistry 27*, 9108−9112.
11. Behe, M. J. (1995) An overabundance of long oligopurine tracts occurs in the genome of simple and complex eukaryotes, *Nucleic Acids Res. 23*, 689−695.
12. Manor, H., Rao, B. S., and Martin, R. G. (1988) Abundance and degree of dispersion of genomic $d(GA)_n.d(TC)_n$ sequences, *J. Mol. Evol. 27*, 96−101.
13. Lee, J. S., Woodsworth, M. L., Latimer, L. J., and Morgan, A. R. (1984) Poly(pyrimidine)·poly(purine) synthetic DNAs containing 5-methylcytosine form stable triplexes at neutral pH, *Nucleic Acids Res. 12*, 6603−6614.
14. Roberts, R. W., and Crothers, D. M. (1992) Stability and properties of double and triple helices: dramatic effects of RNA or DNA backbone composition, *Science 258*, 1463−1466.
15. Escude, C., Sun, J. S., Rougee, M., Garestier, T., and Helene, C. (1992) Stable triple helices are formed upon binding of RNA oligonucleotides and their 2′-O-methyl derivatives to double-helical DNA, *C. R. Acad. Sci., Ser. III 315*, 521−525.
16. Asensio, J. L., Carr, R., Brown, T., and Lane, A. N. (1999) Conformational and thermodynamic properties of parallel intramolecular triple helixes containing a DNA, RNA, or 2′-OMeDNA third strand, *J. Am. Chem. Soc. 121*, 11063−11070.
17. Shimizu, M., Konishi, A., Shimada, Y., Inoue, H., and Ohtsuka, E. (1992) Oligo(2′-O-methyl)ribonucleotides. Effective probes for duplex DN, *FEBS Lett. 302*, 155−158.
18. Cuenoud, B., Casset, F., Husken, D., Natt, F., Wolf, R. M., Altmann, K. H., Martin, P., and Moser, H. E. (1998) Dual recognition of double stranded DNA by 2′-aminoethoxy-modified oligonucleotides, *Angew. Chem., Int. Ed. 37*, 1288−1291.
19. Blommers, M. J., Natt, F., Jahnke, W., and Cuenoud, B. (1998) Dual recognition of double-stranded DNA by 2′-aminoethoxy-modified oligonucleotides: the solution structure of an intramolecular triplex obtained by NMR spectroscopy, *Biochemistry 37*, 17714−17725.
20. Kamiya, M., Torigoe, H., Shindo, H., and Sarai, A. (1996) Temperature dependence and sequence specificity of DNA triplex formation: an analysis using isothermal titration calorimetry, *J. Am. Chem. Soc. 118*, 4532−4538.
21. Westin, L., Blomquist, P., Milligan, J. F., and Wrange, O. (1995) Triple helix DNA alters nucleosomal histone-DNA interactions and acts as a nucleosome barrier, *Nucleic Acids Res. 23*, 2184−2191.
22. Brown, P. M., and Fox, K. R. (1996) Nucleosome core particles inhibit DNA triple helix formation, *Biochem. J. 319* (Part 2), 607−611.
23. Polach, K. J., and Widom, J. (1995) Mechanism of protein access to specific DNA sequences in chromatin: a dynamic equilibrium model for gene regulation, *J. Mol. Biol. 254*, 130−149.
24. Peterson, C. L. (2002) Chromatin remodeling: nucleosomes bulging at the seams, *Curr. Biol. 12*, R245−R247.
25. Jenuwein, T., and Allis, C. D. (2001) Translating the histone code, *Science 293*, 1074−1080.
26. Ahmad, K., and Henikoff, S. (2002) Epigenetic consequences of nucleosome dynamics, *Cell 111*, 281−284.
27. Macris, M. A., and Glazer, P. M. (2002) Transcription dependence of chromosomal gene targeting by triplex-forming oligonucleotides, *J. Biol. Chem. 278*, 3357−3362.
28. Lin, F. L., Majumdar, A., Klotz, L. C., Reszka, A. P., Neidle, S., and Seidman, M. M. (2000) Stability of DNA Triplexes on Shuttle Vector Plasmids in the Replication Pool in Mammalian Cells, *J. Biol. Chem. 275*, 39117−39124.
29. Puri, N., Majumdar, A., Cuenoud, B., Natt, F., Martin, P., Boyd, A., Miller, P. S., and Seidman, M. M. (2001) Targeted gene knockout by 2′-O-aminoethyl modified triplex forming oligonucleotides, *J. Biol. Chem. 276*, 28991−28998.
30. Kopel, V., Pozner, A., Baran, N., and Manor, H. (1996) Unwinding of the third strand of a DNA triple helix, a novel activity of the SV40 large T-antigen helicase, *Nucleic Acids Res. 24*, 330−335.
31. Brosh, R. M., Jr., Majumdar, A., Desai, S., Hickson, I. D., Bohr, V. A., and Seidman, M. M. (2001) Unwinding of a DNA triple helix by the Werner and Bloom syndrome helicases, *J. Biol. Chem. 276*, 3024−3030.
32. Saha, A., Wittmeyer, J., and Cairns, B. R. (2002) Chromatin remodeling by RSC involves ATP-dependent DNA translocation, *Genes Dev. 16*, 2120−2134.
33. Manoharan, M., Prakash, T. P., Barber-Peoc'h, I., Bhat, B., Vasquez, G., Ross, B. S., and Cook, P. D. (1999) N-(2-Cyanoethoxycarbonyloxy)succinimide: a new reagent for protection of amino groups in oligonucleotides, *J. Org. Chem. 64*, 6468−6472.
34. Xodo, L. E. (1995) Kinetic analysis of triple-helix formation by pyrimidine oligodeoxynucleotides and duplex DNA, *Eur. J. Biochem. 228*, 918−926.
35. Arya, D. P., Coffee, R. L., Jr., and Charles, I. (2001) Neomycin-induced hybrid triplex formation, *J. Am. Chem. Soc. 123*, 11093−11094.
36. Sawai, M., Takase, K., Teraoka, H., and Tsukada, K. (1990) Reversible G1 arrest in the cell cycle of human lymphoid cell lines by dimethyl sulfoxide, *Exp. Cell Res. 187*, 4−10.
37. Orren, D. K., Petersen, L. N., and Bohr, V. A. (1997) Persistent DNA damage inhibits S-phase and G2 progression, and results in apoptosis, *Mol. Biol. Cell 8*, 1129−1142.
38. Seidman, M. M., Dixon, K., Razzaque, A., Zagursky, R. J., and Berman, M. L. (1985) A shuttle vector plasmid for studying carcinogen-induced point mutations in mammalian cells, *Gene 38*, 233−237.
39. Manzini, G., Xodo, L. E., Gasparotto, D., Quadrifoglio, F., van der Marel, G. A., and van Boom, J. H. (1990) Triple helix formation by oligopurine-oligopyrimidine DNA fragments. Electrophoretic and thermodynamic behavior, *J. Mol. Biol. 213*, 833−843.
40. Blume, S. W., Lebowitz, J., Zacharias, W., Guarcello, V., Mayfield, C. A., Ebbinghaus, S. W., Bates, P., Jones, D. E., Jr., Trent, J., Vigneswaran, N., and Miller, D. M. (1999) The integral divalent cation within the intermolecular purine*purine·pyrimidine structure: a variable determinant of the potential for and characteristics of the triple helical association, *Nucleic Acids Res. 27*, 695−702.
41. Hartwig, A. (2001) Role of magnesium in genomic stability, *Mutat. Res. 475*, 113−121.
42. Carlomagno, T., Blommers, M. J., Meiler, J., Cuenoud, B., and Griesinger, C. (2001) Determination of aliphatic side-chain conformation using cross-correlated relaxation: application to an extraordinarily stable 2′-aminoethoxy-modified oligonucleotide triplex, *J. Am. Chem. Soc. 123*, 7364−7370.
43. Rougee, M., Faucon, B., Mergny, J. L., Barcelo, F., Giovannangeli, C., Garestier, T., and Helene, C. (1992) Kinetics and thermodynamics of triple-helix formation: effects of ionic strength and mismatches, *Biochemistry 31*, 9269−9278.
44. Porschke, D., and Eigen, M. (1971) Co-operative non-enzymic base recognition. 3. Kinetics of the helix-coil transition of the oligoribouridylic−oligoriboadenylic acid system and of oligoriboadenylic acid alone at acidic pH, *J. Mol. Biol. 62*, 361−381.

45. McNally, J. G., Muller, W. G., Walker, D., Wolford, R., and Hager, G. L. (2000) The glucocorticoid receptor: rapid exchange with regulatory sites in living cells, *Science 287*, 1262−1265.
46. Hager, G. L., Elbi, C., and Becker, M. (2002) Protein dynamics in the nuclear compartment, *Curr. Opin. Genet. Dev. 12*, 137−141.
47. Belmont, A. (2003) Dynamics of chromatin, proteins, and bodies within the cell nucleus, *Curr. Opin. Cell Biol. 15*, 304−310.
48. Fletcher, T. M., Xiao, N., Mautino, G., Baumann, C. T., Wolford, R., Warren, B. S., and Hager, G. L. (2002) ATP-dependent mobilization of the glucocorticoid receptor during chromatin remodeling, *Mol. Cell. Biol. 22*, 3255−3263.
49. Xue, Y., Gibbons, R., Yan, Z., Yang, D., McDowell, T. L., Sechi, S., Qin, J., Zhou, S., Higgs, D., and Wang, W. (2003) The ATRX syndrome protein forms a chromatin-remodeling complex with Daxx and localizes in promyelocytic leukemia nuclear bodies, *Proc. Natl. Acad. Sci. U.S.A. 100*, 10635−10640.
50. Lawrence, J. B., and Hager, G. L. (2003) Nucleus and gene expression: motion meets architecture, *Curr. Opin. Cell Biol. 15*, 255−258.
51. Platani, M., Goldberg, I., Lamond, A. I., and Swedlow, J. R. (2002) Cajal body dynamics and association with chromatin are ATP-dependent, *Nat. Cell Biol. 4*, 502−508.
52. Bijapur, J., Keppler, M. D., Bergqvist, S., Brown, T., and Fox, K. R. (1999) 5-(1-Propargylamino)-2′-deoxyuridine (UP): a novel thymidine analogue for generating DNA triplexes with increased stability, *Nucleic Acids Res. 27*, 1802−1809.
53. Sollogoub, M., Darby, R. A., Cuenoud, B., Brown, T., and Fox, K. R. (2002) Stable DNA Triple Helix Formation Using Oligonucleotides Containing 2′-Aminoethoxy-5-propargylamino-U, *Biochemistry 41*, 7224−7231.
54. Dagle, J. M., and Weeks, D. L. (1996) Positively charged oligonucleotides overcome potassium-mediated inhibition of triplex DNA formation, *Nucleic Acids Res. 24*, 2143−2149.
55. Li, J. S., Fan, Y. H., Zhang, Y., Marky, L. A., and Gold, B. (2003) Design of triple helix forming C-glycoside molecules, *J. Am. Chem. Soc. 125*, 2084−2093.

BI035808L